Impact of $Z \to \eta_{c,b} + g + g$ on the inclusive $\eta_{c,b}$ meson yield in Z-boson decay

Zhan Sun,* Xuan Luo, and Ying-Zhao Jiang

Department of Physics, Guizhou Minzu University, Guiyang 550025, People's Republic of China

(Received 1 December 2021; accepted 15 July 2022; published 1 August 2022)

In this paper, we carry out the next-to-leading-order QCD corrections to $Z \to \eta_Q + g + g (Q = c, b)$ (labeled as gg) through the color-singlet (CS) state of $Q\bar{Q}[^1S_0^{[1]}]$, with the aim of assessing the impact of this process on Z bosons decaying into inclusive η_Q. We find that the QCD corrections to the gg process can notably enhance its leading-order results, especially for the η_c case, which would then greatly increase the existing predictions of $\Gamma_{Z\to\eta_Q+X}$ given by the CS-dominant process $Z \to \eta_Q[^1S_0^{[1]}] + Q + \bar{Q}$. Moreover, with these significant QCD corrections, the gg process would exert crucial influence on the CS-predicted η_Q energy distributions. In conclusion, in the CS studies of $Z \to \eta_Q + X$, besides $Z \to \eta_Q[^1S_0^{[1]}] + Q + \bar{Q}$, $Z \to \eta_Q[^1S_0^{[1]}] + g + g$ can provide phenomenologically indispensable contributions as well.

DOI: 10.1103/PhysRevD.106.034001

I. INTRODUCTION

Due to experimental reconstruction difficulties,[1] the observation of the η_c meson is scant compared to that of J/ψ. For example, HERA, LEP II, and B factories have accumulated copious J/ψ yield data, but they have not yet detected any evident event of inclusive η_c production. In 2014, the LHC (LHCb group), which runs with a large center-of-mass proton-proton collision energy and a high luminosity, achieved the first measurement of inclusive η_c yield [1]. Compared to the theoretical results [2–13], the measured cross sections seem to almost be saturated by the color-singlet (CS) predictions alone, leaving very limited room for the color-octet contributions, and thus posing a serious challenge to the nonrelativistic QCD (NRQCD) factorization [14]; however, Refs. [5,6] point out that NRQCD is still valid in describing the LHCb data. Note that there are large uncertainties in the LHCb released data [1]. Therefore, more studies of inclusive η_c yield in other processes and experiments with better precision are required to further assess the validity of NRQCD in η_c production.

Heavy-quarkonium production in Z-boson decay, which has triggered extensive studies [15–41], provides a good chance for studying the η_c production mechanism. At the LHC, a large number of Z events ($\sim 10^9$/year [33]) can be generated in one running year, with which the study of Z decaying into heavy quarkonium has been an increasingly important area [42–44]. Furthermore, the upgrades of HE (L)-LHC will give birth to a higher collision energy (luminosity), largely improving the accumulated Z yield events. In addition, the proposed future e^+e^- collider, CEPC [45], equipped with a "clean" background and an enormous number of Z production events ($\sim 10^{12}$/year), would also be beneficial for hunting Z decaying into inclusive η_c. From these perspectives, a precise measurement of $Z \to \eta_c + X$ looks promising, and the theoretical study of this process through the CS mechanism could help to explore whether the compatibility of the CS predictions with future measurements still holds.

In $Z \to \eta_c + X$, there exist two CS processes contributing at leading-order (LO) accuracy in α_s: i.e., $Z \to \eta_c[^1S_0^{[1]}] + c + \bar{c}$ (labeled as $c\bar{c}$) and $Z \to \eta_c[^1S_0^{[1]}] + g + g$ (labeled as gg). We can learn from Refs. [17,18] that the $c\bar{c}$ process plays a leading role in the CS LO predictions because of the c-quark fragmentation; owing to the suppression of $\frac{m_c^2}{m_Z^2}$ [18], the gg process contributes just slightly at LO (less than 5% of $\Gamma_{c\bar{c}}$). However, considering the advent of the gluon-fragmentation structures in the next-to-leading-order (NLO) calculations of $Z \to \eta_c + g + g$—i.e., $Z \to q + \bar{q} + g^*$; $g^* \to \eta_c + g$ ($q = u, d, s$) and the loop-induced process $Z \to g + g^*; g^* \to \eta_c + g$—the uncalculated QCD corrections to the gg process are expected to provide considerable contributions. In addition, the η_c energy distributions in the gg and $c\bar{c}$ processes may thoroughly be different. The gg process, together with the QCD corrections, are strongly suppressed by the factor $\frac{M_{\eta_c}^2}{E_{\eta_c}^2}$ for large z [26,46,47], and thereby the z value corresponding to the largest $\frac{d\Gamma}{dz}$ should be

*zhansun@cqu.edu.cn

[1] η_c is always established by its decay into multiple hadrons, such as $p\bar{p}$, which is more difficult than the J/ψ detection.

small; regarding the $c\bar{c}$ process, as a result of the c-quark fragmentation, the dominant contributions exist in the large-z region [18]. In view of these points, $Z \to \eta_c[^1S_0^{[1]}] + g + g$ would be phenomenologically crucial for the inclusive η_c yield in Z decay.

In contrast with η_c, the larger mass of η_b would result in a smaller typical coupling constant and relative velocity (v) between the constituent $b\bar{b}$ quarks, subsequently leading to better convergent results over the expansion in α_s and v. On the experimental side, however, η_b has so far been observed only in e^+e^- annihilation [48–51]. Taken together, in this article we will carry out the first NLO QCD corrections to $Z \to \eta_c(\eta_b)[^1S_0^{[1]}] + g + g$, so as to provide a deeper insight into the $\eta_c(\eta_b)$ production mechanism.

The rest of the paper is organized as follows: In Sec. II, we give a description of the calculation formalism. In Sec. III, the phenomenological results and discussions are presented. Section IV is reserved as a summary.

II. CALCULATION FORMALISM

Within the NRQCD framework [14,52], the decay width of $Z \to \eta_Q + X (Q = c, b)$ can be factorized as

$$\Gamma = \hat{\Gamma}_{Z\to Q\bar{Q}[n]+X}\langle \mathcal{O}^{\eta_Q}(n)\rangle, \tag{1}$$

where $\hat{\Gamma}$ are the perturbative calculable short distance coefficients (SDCs), representing the inclusive production of a configuration of the $Q\bar{Q}[n]$ intermediate state. The universal nonperturbative long-distance matrix element $\langle \mathcal{O}^{\eta_Q}(n)\rangle$ stands for the probability of $Q\bar{Q}[n]$ into η_Q. In this paper, we focus only on the CS contributions, and accordingly n takes on $^1S_0^{[1]}$. The LO process of $Z \to Q\bar{Q}[^1S_0^{[1]}] + Q + \bar{Q}$, which is introduced as a comparison and which is free of divergence, has been calculated in Ref. [17]; in the following, we only describe the calculation formalism of $Z \to Q\bar{Q}[^1S_0^{[1]}] + g + g$ up to the NLO QCD accuracy.

A. LO

The LO SDCs can be expressed as

$$\hat{\Gamma}_{\mathrm{LO}} = \int |\mathcal{M}|^2 d\Pi_3, \tag{2}$$

where $|\mathcal{M}|^2$ is the squared amplitude, and $d\Pi_3$ is the standard three-body phase space.

According to Fig. 1, $\mathcal{M}_1$ can be written as

$$\mathcal{M}_1 = \kappa \times \mathrm{Tr}\left[\not{\epsilon}(p_1)(\xi_1 P_L + \xi_2 P_R)\frac{-\not{p}_{22} - \not{p}_3 - \not{p}_4 + m_Q}{(p_{22}+p_3+p_4)^2 - m_Q^2} \times \not{\epsilon}(p_4)\frac{-\not{p}_{22} - \not{p}_3 + m_Q}{(p_{22}+p_3)^2 - m_Q^2}\not{\epsilon}(p_3)\Pi^0_{Q\bar{Q}}(p_2)\right], \tag{3}$$

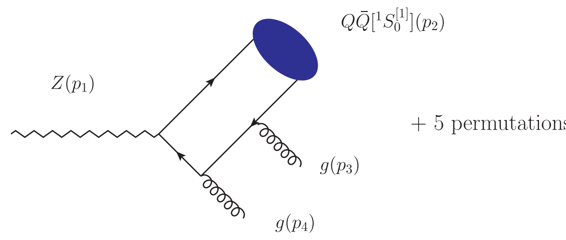

FIG. 1. Typical LO Feynman diagrams of $Z \to Q\bar{Q}[^1S_0^{[1]}] + g + g$ $(Q = c, b)$.

where $\kappa = \mathcal{C}\frac{e g_s^2}{4\sin\theta_{\mathrm{w}}\cos\theta_{\mathrm{w}}}$, with $\mathcal{C}$ being the color factor. $\epsilon(p_1)$ and $\epsilon(p_{3(4)})$ are the polarization vectors of the initial Z boson and the final-state gluons, respectively. $P_L = (1-\gamma^5)/2$ and $P_R = (1+\gamma^5)/2$; $\xi_1 = 2 - \frac{8}{3}\sin^2\theta_w$ and $\xi_2 = -\frac{8}{3}\sin^2\theta_w$ for the $Z_{c\bar{c}}$ vertex, while $\xi_1 = 2 - \frac{4}{3}\sin^2\theta_w$ and $\xi_2 = -\frac{4}{3}\sin^2\theta_w$ for the $Z_{b\bar{b}}$ vertex.

The momenta of the constituent quarks follow as

$$p_{21} = \frac{m_Q}{M_{Q\bar{Q}}}p_2 + q \quad \text{and} \quad p_{22} = \frac{m_Q}{M_{Q\bar{Q}}}p_2 - q, \tag{4}$$

where $m_{Q(\bar{Q})} = M_{Q\bar{Q}}/2$ is implicitly adopted to ensure the gauge invariance of the hard scattering amplitude; $q(\simeq 0)$ is the relative momentum between the two constituent heavy quarks inside the quarkonium.

The covariant form of the projector $\Pi^0_{Q\bar{Q}}$ reads

$$\Pi^0_{Q\bar{Q}}(p_2) = \frac{1}{\sqrt{8m_Q^3}}(\not{p}_{22} - m_{\bar{Q}})\gamma^5(\not{p}_{21} + m_Q). \tag{5}$$

In a similar way, the amplitudes $\mathcal{M}_2, \ldots, \mathcal{M}_6$ can be derived by permutations. By squaring the sum of all six amplitudes and summing over the polarization vectors of the Z boson and the two final gluons, we finally obtain the squared amplitude $|\mathcal{M}|^2$.

B. NLO

Up to NLO in α_s, the SDCs comprise three contributing components,

$$\hat{\Gamma}_{\mathrm{NLO}} = \hat{\Gamma}_{\mathrm{Born}} + \hat{\Gamma}_{\mathrm{Virtual}} + \hat{\Gamma}_{\mathrm{Real}}, \tag{6}$$

where $\hat{\Gamma}_{\mathrm{Born}}$ refers to the tree-level process and $\hat{\Gamma}_{\mathrm{Virtual(Real)}}$ is the virtual (real) correction.

1. Virtual corrections

The virtual corrections are composed of the contributions of the one-loop ($\hat{\Gamma}_{\mathrm{Loop}}$) and counterterm ($\hat{\Gamma}_{\mathrm{CT}}$) diagrams, as representatively shown in Fig. 2. $\hat{\Gamma}_{\mathrm{Virtual}}$ can accordingly be expressed as

$$\hat{\Gamma}_{\mathrm{Virtual}} = \hat{\Gamma}_{\mathrm{Loop}} + \hat{\Gamma}_{\mathrm{CT}}. \tag{7}$$

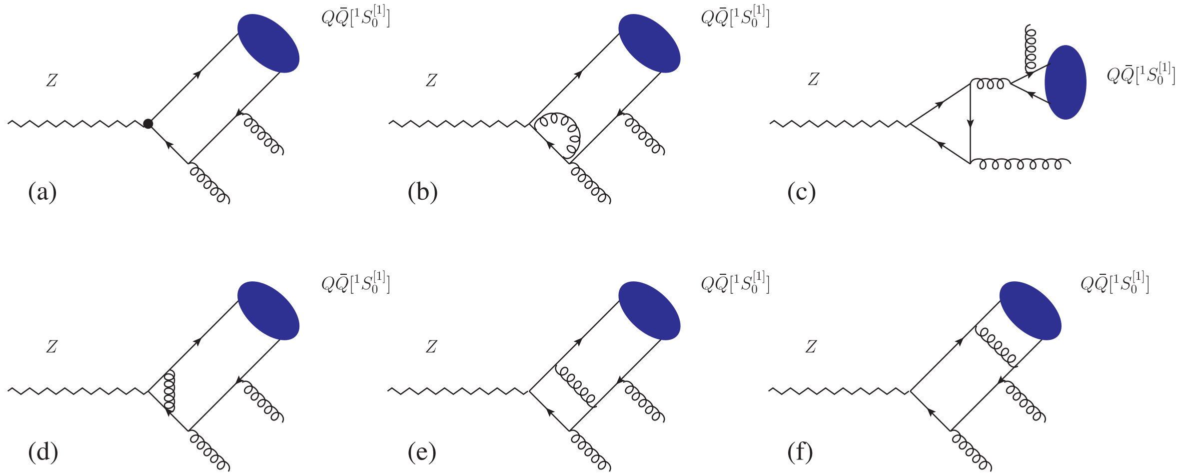

FIG. 2. Representative Feynman diagrams of the virtual corrections to $Z \to Q\bar{Q}[^1S_0^{[1]}] + g + g$ ($Q = c$, b).

To isolate the ultraviolet (UV) and infrared (IR) divergences, we adopt the dimensional regularization with $D = 4 - 2\epsilon$. The on-mass-shell (OS) scheme is employed to set the renormalization constants for the heavy quark mass (Z_m), heavy quark filed (Z_2), and gluon field (Z_3). The modified minimal-subtraction ($\overline{\mathrm{MS}}$) scheme is used for the QCD gauge coupling (Z_g). The renormalization constants read ($Q = c$, b)

$$\begin{aligned}
\delta Z_m^{OS} &= -3C_F \frac{\alpha_s}{4\pi}\left[\frac{1}{\epsilon_{\mathrm{UV}}} - \gamma_E + \ln\frac{4\pi\mu_r^2}{m_Q^2} + \frac{4}{3}\right],\\
\delta Z_2^{OS} &= -C_F \frac{\alpha_s}{4\pi}\left[\frac{1}{\epsilon_{\mathrm{UV}}} + \frac{2}{\epsilon_{\mathrm{IR}}} - 3\gamma_E + 3\ln\frac{4\pi\mu_r^2}{m_Q^2} + 4\right],\\
\delta Z_3^{OS} &= \frac{\alpha_s}{4\pi}\left[(\beta_0' - 2C_A)\left(\frac{1}{\epsilon_{\mathrm{UV}}} - \frac{1}{\epsilon_{\mathrm{IR}}}\right)\right.\\
&\quad - \frac{4}{3}T_F\left(\frac{1}{\epsilon_{\mathrm{UV}}} - \gamma_E + \ln\frac{4\pi\mu_r^2}{m_c^2}\right)\\
&\quad \left. - \frac{4}{3}T_F\left(\frac{1}{\epsilon_{\mathrm{UV}}} - \gamma_E + \ln\frac{4\pi\mu_r^2}{m_b^2}\right)\right],\\
\delta Z_g^{\overline{\mathrm{MS}}} &= -\frac{\beta_0}{2}\frac{\alpha_s}{4\pi}\left[\frac{1}{\epsilon_{\mathrm{UV}}} - \gamma_E + \ln(4\pi)\right],
\end{aligned} \tag{8}$$

where γ_E is the Euler's constant, $\beta_0 (= \frac{11}{3}C_A - \frac{4}{3}T_F n_f)$ is the one-loop coefficient of the β function, and $\beta_0' = \frac{11}{3}C_A - \frac{4}{3}T_F n_{lf}$. $n_f (= 5)$ and $n_{lf} (= n_f - 2)$ are the numbers of active quark flavors and light quark flavors, respectively. In SU(3), the color factors are given by $T_F = \frac{1}{2}$, $C_F = \frac{4}{3}$, and $C_A = 3$.

In calculating $\hat{\Gamma}_{\mathrm{Loop}}$, we use FeynArts [53] to generate all the involved one-loop diagrams and the corresponding analytical amplitudes; then the package FeynCalc [54] is applied to tackle the traces of the γ and color matrices such that the hard-scattering amplitudes are transformed into expressions with loop integrals. Note that the D-dimension γ traces in $\hat{\Gamma}_{\mathrm{Loop}}$ involve the γ_5 matrix, and we adopt the following scheme [28,30,55] to deal with it:

(i) For Figs. 2(a), 2(b), and 2(d)–2(f), which contain two γ_5 matrices, we move the two γ_5 together and then obtain an identity matrix by $\gamma_5^2 = 1$.

(ii) For the triangle anomalous diagram—i.e., Fig. 2(c)—we choose the same starting point (Z-vertex) to write down the amplitudes without the implementation of cyclicity.

In the next step, we utilize our self-written *Mathematica* codes with the implementations of Apart [56] and FIRE [57] to reduce these loop integrals to a set of irreducible master integrals, which would be numerically evaluated by using the package LoopTools [58].

2. Real corrections

The real corrections to $Z \to Q\bar{Q}[^1S_0^{[1]}] + g + g$ involve two $1 \to 4$ processes ($q = u$, d, s),

$$\begin{aligned}
&Z \to Q\bar{Q}[^1S_0^{[1]}] + g + g + g,\\
&Z \to Q\bar{Q}[^1S_0^{[1]}] + g + q + \bar{q},
\end{aligned} \tag{9}$$

whose representative Feynman diagrams are displayed in Fig. 3. Note that, in calculating $Z \to Q\bar{Q}[^1S_0^{[1]}] + g + g + g$, we apply the physical polarization tensor,[2] $P_{\mu\nu}$, for the polarization summation of the final gluons, thereby avoiding the consideration of the ghost diagrams.

The phase-space integrations of the two processes in Eq. (9) would generate IR singularities, which can be isolated by slicing the phase space into different regions—namely, the two-cutoff slicing strategy [59]. By introducing

[2] $P_{\mu\nu} = -g_{\mu\nu} + \frac{k_\mu \eta_\mu + k_\nu \eta_\mu}{k\cdot\eta}$, where k is the momentum of one of the three final gluons, and η is conveniently set as the momentum of one of the other two gluons in the final state.

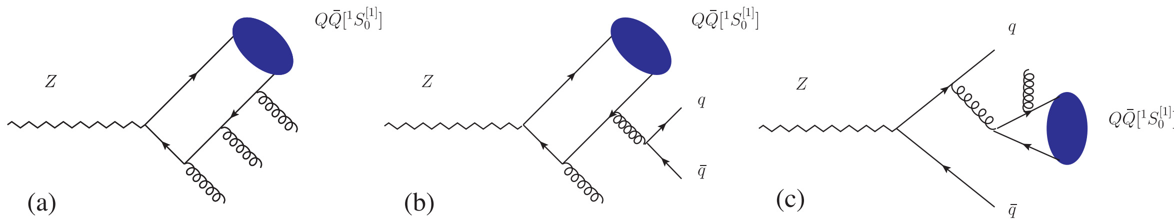

FIG. 3. Representative Feynman diagrams of the real corrections to $Z \to Q\bar{Q}[^1S_0^{[1]}] + g + g$ ($Q = c, b$). "q" denotes the light quarks (u, d, s).

two small cutoff parameters (δ_s and δ_c) to decompose the phase space into three parts, $\hat{\Gamma}_{\rm Real}$ can then be written as

$$\hat{\Gamma}_{\rm Real} = \hat{\Gamma}_{\rm S} + \hat{\Gamma}_{\rm HC} + \hat{\Gamma}_{\rm H\bar{C}}. \tag{10}$$

$\hat{\Gamma}_{\rm S}$ are the soft terms arsing only from $Z \to Q\bar{Q}[^1S_0^{[1]}] + g + g + g$; $\hat{\Gamma}_{\rm HC}$ denotes the hard-collinear terms, which originate from both the two processes in Eq. (9). The hard-noncollinear terms $\hat{\Gamma}_{\rm H\bar{C}}$ are finite, and we use the FDC package [60] to compute them numerically by means of standard Monte Carlo integration techniques. With the cancellation of the dependences of $\hat{\Gamma}_{\rm S} + \hat{\Gamma}_{\rm HC}$ and $\hat{\Gamma}_{\rm H\bar{C}}$ on $\delta_{s,c}$, the $\hat{\Gamma}_{\rm Real}$ would eventually be independent of the cutoff parameters.

By summing up $\Gamma_{\rm Virtual}$ and $\Gamma_{\rm Real}$, all the divergences involved in the NLO calculations would eventually be canceled, and in the following, we will perform the numerical calculations.

III. PHENOMENOLOGICAL RESULTS

Under the approximation of $m_{Q(\bar{Q})} = M_{\eta_Q}/2$ ($Q = c, b$), the quark masses are taken as $m_c = 1.5$ GeV and $m_b = 4.7$ GeV [61]. The other input parameters are set as

$$m_Z = 91.1876\ \text{GeV}, \qquad m_{q/\bar{q}} = 0 \quad (q = u, d, s),$$
$$\sin^2\theta_W = 0.226, \qquad \alpha = 1/128. \tag{11}$$

To determine $\langle \mathcal{O}^{\eta_Q}(^1S_0^{[1]}) \rangle$, we employ the relations to the radial wave functions at the origin,

$$\frac{\langle \mathcal{O}^{\eta_Q}(^1S_0^{[1]}) \rangle}{2N_c} = \frac{1}{4\pi} |R_{\eta_Q}(0)|^2, \tag{12}$$

where $|R_{\eta_Q}(0)|^2$ reads [62]

$$|R_{\eta_c}(0)|^2 = 0.81\ \text{GeV}^3,$$
$$|R_{\eta_b}(0)|^2 = 6.477\ \text{GeV}^3. \tag{13}$$

We summarize the predicted decay widths of $Z \to \eta_Q + g + g$ in Tables I and II. Inspecting the two tables, one can observe

(i) For $Z \to \eta_c + g + g$, $\Gamma_{\rm Vir+S+HC}$ severely cancels the large contribution of $\Gamma^{ggg}_{\rm H\bar{C}}$; the other part in $\Gamma_{\rm H\bar{C}}$—i.e., $\Gamma^{gq\bar{q}}_{\rm H\bar{C}}$, which is dominated by the significant contributions of the gluon-fragmentation structures [Fig. 3(c); cf. $\Gamma^{gq\bar{q}}_{\rm frag}$ in Table I]—is comparable with $\Gamma^{ggg}_{\rm H\bar{C}}$ and then enhances the LO results to an extremely large extent, as pictorially shown in the left panel of Fig. 4. In other words, the large K factors in Table I can mainly be attributed to the contributions of Fig. 3(c), which is gauge invariant and free of divergences. $\Gamma_{\rm NLO}$ appears to be more sensitive than $\Gamma_{\rm LO}$ on the choice of the c-quark mass, which can be understood by the fact that the dominant gluon-fragmentation contributions in $\Gamma^{gq\bar{q}}_{\rm H\bar{C}}$ depend heavily on the value of m_c.

(ii) As for η_b, there still holds a severe cancellation between $\Gamma_{\rm Vir+S+HC}$ and $\Gamma^{ggg}_{\rm H\bar{C}}$; however, since the impact of the gluon-fragmentation structure,

TABLE I. Decay widths (in units of KeV) of $Z \to \eta_c + g + g$ corresponding to different m_c (units: GeV). The superscripts "ggg" and "$gq\bar{q}$" stand for $Z \to c\bar{c}[^1S_0^{[1]}] + g + g + g$ and $Z \to c\bar{c}[^1S_0^{[1]}] + g + q + \bar{q}$, respectively; "v(av)" for the (axial-)vector part; and "frag" for the processes in Fig. 3(c). K is identical to $\Gamma_{\rm NLO}/\Gamma_{\rm LO}$. The cutoff parameters are taken as $\delta_s = 1 \times 10^{-3}$ and $\delta_c = 2 \times 10^{-5}$.

μ_r	m_c	α_s	$\Gamma_{\rm LO}$	$\Gamma_{\rm Vir+S+HC}$	$\Gamma^{ggg}_{\rm H\bar{C}}$	$\Gamma^{gq\bar{q}_{\rm av}}_{\rm H\bar{C}}$	$\Gamma^{gq\bar{q}_{\rm v}}_{\rm H\bar{C}}$	$\Gamma_{\rm NLO}$	K	$\Gamma^{gq\bar{q}}_{\rm frag}$
$2m_c$	1.4	0.26573	5.721	−110.2	104.8	69.54	25.04	94.89	16.6	91.31
	1.5	0.25864	4.828	−90.29	85.97	49.22	17.58	67.31	13.9	64.08
	1.6	0.25235	4.123	−75.01	71.43	35.70	12.64	48.88	11.9	46.07
m_Z	1.4	0.11916	1.150	−8.772	9.455	6.270	2.258	10.36	9.01	8.233
	1.5	0.11916	1.025	−7.812	8.401	4.814	1.719	8.147	7.95	6.270
	1.6	0.11916	0.919	−7.002	7.521	3.759	1.330	6.527	7.10	4.851

TABLE II. Decay widths (in units of KeV) of $Z \to \eta_b + g + g$ corresponding to different m_b's (units: GeV). The superscripts "ggg" and "$gq\bar{q}$" stand for $Z \to b\bar{b}[^1S_0^{[1]}] + g + g + g$ and $Z \to b\bar{b}[^1S_0^{[1]}] + g + q + \bar{q}$, respectively; "v(av)" for the (axial-)vector part; and "frag" for the processes in Fig. 3(c). K is identical to $\Gamma_{\rm NLO}/\Gamma_{\rm LO}$. The cutoff parameters are taken as $\delta_s = 1 \times 10^{-3}$ and $\delta_c = 2 \times 10^{-5}$.

μ_r	m_b	α_s	$\Gamma_{\rm LO}$	$\Gamma_{\rm Vir+S+HC}$	$\Gamma^{ggg}_{\rm H\bar{C}}$	$\Gamma^{gq\bar{q}_{\rm av}}_{\rm H\bar{C}}$	$\Gamma^{gq\bar{q}_{\rm v}}_{\rm H\bar{C}}$	$\Gamma_{\rm NLO}$	K	$\Gamma^{gq\bar{q}}_{\rm frag}$
$2m_b$	4.6	0.18422	2.515	−31.35	29.94	2.192	0.420	3.717	1.48	1.533
	4.7	0.18326	2.383	−29.49	28.17	2.007	0.374	3.444	1.44	1.363
	4.8	0.18234	2.260	−27.77	26.52	1.843	0.333	3.186	1.41	1.215
m_Z	4.6	0.11916	1.052	−7.783	8.103	0.593	0.114	2.079	1.98	0.415
	4.7	0.11916	1.007	−7.440	7.742	0.552	0.103	1.964	1.95	0.374
	4.8	0.11916	0.965	−7.117	7.402	0.514	0.093	1.857	1.92	0.339

$g^* \to \eta_b + g$, is greatly weakened by the large mass of η_b (cf. $\Gamma^{gq\bar{q}}_{\rm frag}$ in Table II), $\Gamma^{gq\bar{q}}_{\rm H\bar{C}}$ contributes just slightly. As a result, the QCD corrections to $Z \to \eta_b + g + g$ appear to be much wilder than the η_c case, which can clearly be seen by the second panel in Fig. 4.

Now, we compare the contributions of $Z \to \eta_Q + g + g$ $(Q = c,\ b)$ with those of $Z \to \eta_Q + Q + \bar{Q}$. Taking $\mu_r = 2m_{c,b}$ with $m_c = 1.5$ GeV and $m_b = 4.7$ GeV, we have

$$\Gamma^{c\bar{c}}_{\rm LO} = 99.90\ \text{KeV},\qquad \Gamma^{b\bar{b}}_{\rm LO} = 12.23\ \text{KeV}, \tag{14}$$

and then

$$\frac{\Gamma^{gg}_{\rm LO}}{\Gamma^{c\bar{c}}_{\rm LO}} = 4.83\%,\qquad \frac{\Gamma^{gg}_{\rm NLO}}{\Gamma^{c\bar{c}}_{\rm LO}} = 67.4\%,$$
$$\frac{\Gamma^{gg}_{\rm LO}}{\Gamma^{b\bar{b}}_{\rm LO}} = 19.5\%,\qquad \frac{\Gamma^{gg}_{\rm NLO}}{\Gamma^{b\bar{b}}_{\rm LO}} = 28.1\%, \tag{15}$$

where "gg" stands for $Z \to \eta_Q + g + g$, and "$Q\bar{Q}$" stands for $Z \to \eta_Q + Q + \bar{Q}$. One can find, after including the newly calculated QCD corrections to $Z \to \eta_Q + g + g$, that the gg process would be comparable with the $Q\bar{Q}$ one.

In Fig. 5, the η_Q energy distributions are drawn with z defined as $\frac{2E_{\eta_Q}}{m_Z}$. It can be seen that

(i) The dominant contributions in $\Gamma^{\rm LO}_{Z\to\eta_c+c+\bar{c}}$ arise from the region of $z \simeq 0.7$, while the peak of $\frac{d\Gamma^{\rm LO}_{Z\to\eta_c+g+g}}{dz}$ lies in the vicinity of $z \simeq 0.2$. By incorporating the QCD corrections, the gg results are notably enhanced, especially at the small- and mid-z regions. As a result, adding the gg contributions would greatly increase the differential decay widths given by $Z \to \eta_c + c + \bar{c}$, which can clearly be seen by the huge discrepancy between the two lines referring to $c\bar{c}_{\rm LO}$ with or without $gg_{\rm NLO}$ in the two upper panels of Fig. 5.

(ii) Regarding η_b, there also exists an evident peak of $\frac{d\Gamma^{\rm LO}_{Z\to\eta_b+b+\bar{b}}}{dz}$ around $z \simeq 0.7$; in $Z \to \eta_b + g + g$ at LO, the mid-z regions ($z \simeq 0.5$) contribute dominantly. With the QCD corrections, the gg process would evidently raise the lines given by $Z \to \eta_b + b + \bar{b}$, as manifested by the large difference in height of the line of $b\bar{b}_{\rm LO}$ and that of $b\bar{b}_{\rm LO} + gg_{\rm NLO}$ in the two lower panels of Fig. 5.

To summarize, our newly calculated QCD corrections to $Z \to \eta_Q[^1S_0^{[1]}] + g + g$ could enormously enhance its LO results, and then greatly elevate the phenomenological significance of the gg process in Z decaying into inclusive η_c.

Inspired by the large contributions of Fig. 3(c), at last, we investigate the significance of $Z \to c\bar{c}[^1S_0^{[1]}] + g + b + \bar{b}$ and $Z \to b\bar{b}[^1S_0^{[1]}] + g + c + \bar{c}$, which also involve the

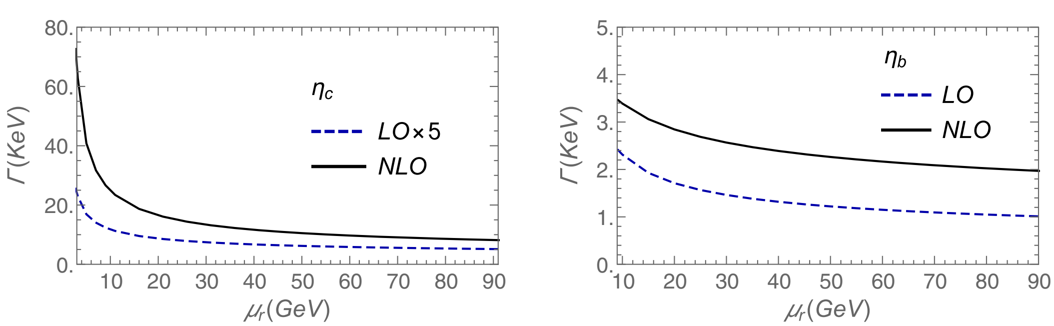

FIG. 4. Decay widths of $Z \to \eta_Q + g + g$ $(Q = c, b)$ as a function of the renormalization scale μ_r. $m_c = 1.5$ GeV and $m_b = 4.7$ GeV.

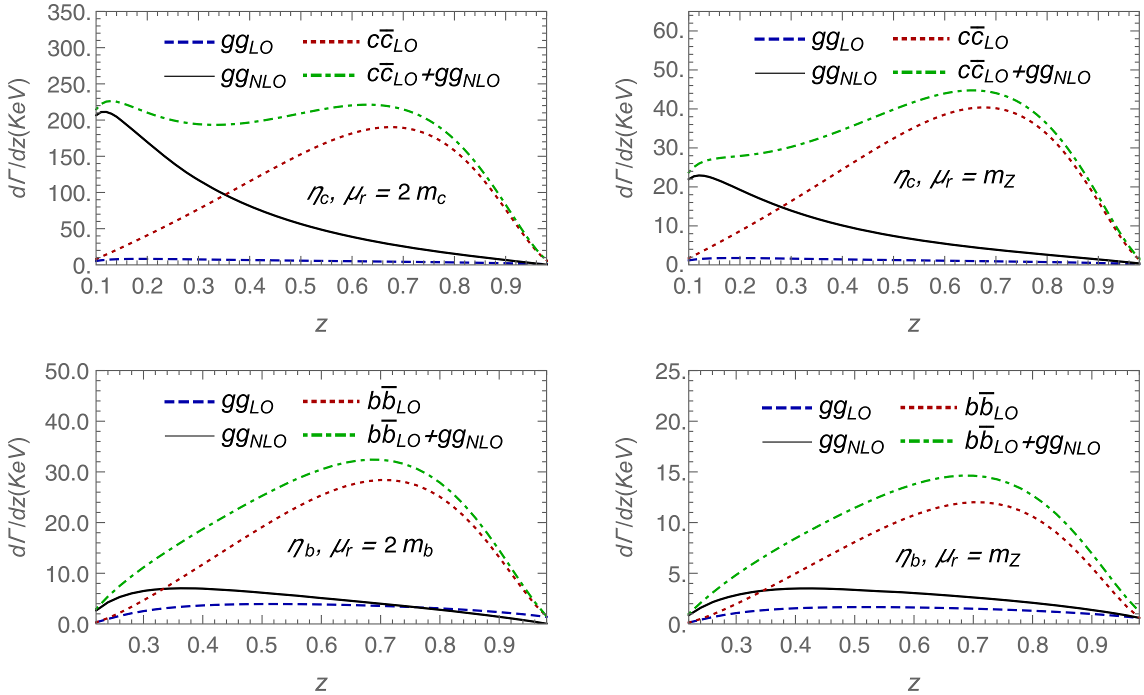

FIG. 5. η_Q ($Q = c$, b) energy distributions with z defined as $\frac{2E_{\eta_Q}}{m_Z}$; "$gg(Q\bar{Q})$" denotes the process of $Z \to \eta_Q + gg(Q\bar{Q})$. $m_c = 1.5$ GeV and $m_b = 4.7$ GeV.

gluon-fragmentation structures.[3] The two processes are free of divergences, and by straightforward calculations under $\mu_r = 2m_{c,b}$ ($m_c = 1.5$ GeV and $m_b = 4.7$ GeV), we have

$$\Gamma_{Z\to c\bar{c}[^1S_0^{[1]}]+g+b+\bar{b}} = 20.01 \text{ KeV},$$
$$\Gamma_{Z\to b\bar{b}[^1S_0^{[1]}]+g+c+\bar{c}} = 0.547 \text{ KeV}. \qquad (16)$$

As compared to Eq. (14), the above two processes are indispensable for the inclusive $\eta_{c,b}$ yield in Z-boson decay.

IV. SUMMARY

In this manuscript, we achieve the first NLO corrections to $Z \to \eta_Q + g + g (Q = c, b)$ through the CS state of $Q\bar{Q}[^1S_0^{[1]}]$. We find that the newly calculated QCD corrections can noticeably enhance its LO results, following which the gg process would contribute comparably to the CS-dominant process $Z \to \eta_Q[^1S_0^{[1]}] + Q + \bar{Q}$. Moreover, with the QCD corrections, the gg process would profoundly influence the existing CS-predicted η_Q energy distribution. Therefore, to arrive at a strict CS prediction of $Z \to \eta_Q + X$, besides $Z \to \eta_Q[^1S_0^{[1]}] + Q + \bar{Q}$, it appears mandatory to take $Z \to \eta_Q[^1S_0^{[1]}] + g + g$ into consideration as well.

[3]The processes of $Z \to c\bar{c}[^1S_0^{[1]}] + g + c + \bar{c}$ and $Z \to b\bar{b}[^1S_0^{[1]}] + g + b + \bar{b}$, which include IR singularities, should be categorized as parts of the real corrections to $Z \to c\bar{c}[^1S_0^{[1]}] + c + \bar{c}$ and $Z \to b\bar{b}[^1S_0^{[1]}] + b + \bar{b}$, respectively.

ACKNOWLEDGMENTS

This work is supported in part by the Natural Science Foundation of China under Grant No. 12065006, and by the Project of GuiZhou Provincial Department of Science and Technology under Grants No. QKHJC[2019]1167. and No. QKHJC[2020]1Y035.

[1] R. Aaij *et al.* (LHCb Collaboration), Measurement of the $\eta_c(1S)$ production cross-section in proton-proton collisions via the decay $\eta_c(1S) \to p\bar{p}$, Eur. Phys. J. C **75**, 311 (2015).
[2] S. S. Biswal and K. Sridhar, η_c production at the Large Hadron Collider, J. Phys. G **39**, 015008 (2012).
[3] A. K. Likhoded, A. V. Luchinsky, and S. V. Poslavsky, Production of η_Q meson at LHC, Mod. Phys. Lett. A **30**, 1550032 (2015).
[4] M. Butenschoen, Z. G. He, and B. A. Kniehl, η_c Production at the LHC Challenges Nonrelativistic-QCD

Factorization, Phys. Rev. Lett. **114**, 092004 (2015).
[5] H. Han, Y. Q. Ma, C. Meng, H. S. Shao, and K. T. Chao, η_c Production at LHC and Indications on the Understanding of J/ψ Production, Phys. Rev. Lett. **114**, 092005 (2015).
[6] H. F. Zhang, Z. Sun, W. L. Sang, and R. Li, Impact of η_c Hadroproduction Data on Charmonium Production and Polarization within NRQCD Framework, Phys. Rev. Lett. **114**, 092006 (2015).
[7] J. P. Lansberg, H. S. Shao, and H. F. Zhang, η_c' Hadroproduction at next-to-leading order and its relevance to ψ' production, Phys. Lett. B **786**, 342 (2018).
[8] S. P. Baranov and A. V. Lipatov, Are there any challenges in the charmonia production and polarization at the LHC?, Phys. Rev. D **100**, 114021 (2019).
[9] I. Babiarz, R. Pasechnik, W. Schäfer, and A. Szczurek, Prompt hadroproduction of $\eta_c(1S, 2S)$ in the k_T-factorization approach, J. High Energy Phys. 02 (2020) 037.
[10] Y. Feng, J. He, J. P. Lansberg, H. S. Shao, A. Usachov, and H. F. Zhang, Phenomenological NLO analysis of η_c production at the LHC in the collider and fixed-target modes, Nucl. Phys. **B945**, 114662 (2019).
[11] J. P. Lansberg, New observables in inclusive production of quarkonia, Phys. Rep. **889**, 1 (2020).
[12] Tichouk, H. Sun, and X. Luo, Hard diffractive $\eta_{\mathrm{c,b}}$ hadroproduction at the LHC, Phys. Rev. D **101**, 054035 (2020).
[13] J. P. Lansberg and M. A. Ozcelik, Curing the unphysical behaviour of NLO quarkonium production at the LHC and its relevance to constrain the gluon PDF at low scales, Eur. Phys. J. C **81**, 497 (2021).
[14] G. T. Bodwin, E. Braaten, and G. P. Lepage, Rigorous QCD analysis of inclusive annihilation and production of heavy quarkonium, Phys. Rev. D **51**, 1125 (1995); Erratum, Phys. Rev. D **55**, 5853 (1997).
[15] B. Guberina, J. H. Kuhn, R. D. Peccei, and R. Ruckl, Rare decays of the Z^0, Nucl. Phys. **B174**, 317 (1980).
[16] W. Y. Keung, Off resonance production of heavy vector quarkonium states in e^+e^- annihilation, Phys. Rev. D **23**, 2072 (1981).
[17] V. D. Barger, K. m. Cheung, and W. Y. Keung, Z-boson decays to heavy quarkonium, Phys. Rev. D **41**, 1541 (1990).
[18] E. Braaten, K. m. Cheung, and T. C. Yuan, Z^0 decay into charmonium via charm quark fragmentation, Phys. Rev. D **48**, 4230 (1993).
[19] S. Fleming, Electromagnetic production of quarkonium in Z^0 decay, Phys. Rev. D **48**, R1914 (1993).
[20] K. m. Cheung, W. Y. Keung, and T. C. Yuan, Color Octet Quarkonium Production at the Z Pole, Phys. Rev. Lett. **76**, 877 (1996).
[21] S. Baek, P. Ko, J. Lee, and H. S. Song, Color octet heavy quarkonium productions in Z^0 decays at LEP, Phys. Lett. B **389**, 609 (1996).
[22] P. L. Cho, Prompt upsilon and psi production at LEP, Phys. Lett. B **368**, 171 (1996).
[23] P. Ernstrom, L. Lonnblad, and M. Vanttinen, Evolution effects in Z^0 fragmentation into charmonium, Z. Phys. C **76**, 515 (1997).
[24] E. M. Gregores, F. Halzen, and O. J. P. Eboli, Prompt charmonium production in Z decays, Phys. Lett. B **395**, 113 (1997).
[25] C. f. Qiao, F. Yuan, and K. T. Chao, A crucial test for color octet production mechanism in Z^0 decays, Phys. Rev. D **55**, 4001 (1997).
[26] C. G. Boyd, A. K. Leibovich, and I. Z. Rothstein, J/ψ production at LEP: Revisited and resummed, Phys. Rev. D **59**, 054016 (1999).
[27] L. C. Deng, X. G. Wu, Z. Yang, Z. Y. Fang, and Q. L. Liao, Z_0-boson decays to $B_c^{(*)}$ meson and its uncertainties, Eur. Phys. J. C **70**, 113 (2010).
[28] R. Li and J. X. Wang, The next-to-leading-order QCD correction to inclusive $J/\psi(\Upsilon)$ production in Z^0 decay, Phys. Rev. D **82**, 054006 (2010).
[29] Z. Yang, X. G. Wu, L. C. Deng, J. W. Zhang, and G. Chen, Production of the P-wave excited B_c-states through the Z^0-boson decays, Eur. Phys. J. C **71**, 1563 (2011).
[30] C. F. Qiao, L. P. Sun, and R. L. Zhu, The NLO QCD corrections to B_c meson production in Z^0 decays, J. High Energy Phys. 08 (2011) 131.
[31] T. C. Huang and F. Petriello, Rare exclusive decays of the Z-boson revisited, Phys. Rev. D **92**, 014007 (2015).
[32] J. Jiang, L. B. Chen, and C. F. Qiao, QCD NLO corrections to inclusive B_c^* production in Z^0 decays, Phys. Rev. D **91**, 034033 (2015).
[33] Q. L. Liao, Y. Yu, Y. Deng, G. Y. Xie, and G. C. Wang, Excited heavy quarkonium production via Z^0 decays at a high luminosity collider, Phys. Rev. D **91**, 114030 (2015).
[34] G. T. Bodwin, H. S. Chung, J. H. Ee, and J. Lee, Z-boson decays to a vector quarkonium plus a photon, Phys. Rev. D **97**, 016009 (2018).
[35] A. K. Likhoded and A. V. Luchinsky, Double charmonia production in exclusive Z-boson decays, Mod. Phys. Lett. A **33**, 1850078 (2018).
[36] Z. Sun and H. F. Zhang, Next-to-leading-order QCD corrections to the decay of Z boson into $\chi_c(\chi_b)$, Phys. Rev. D **99**, 094009 (2019).
[37] H. S. Chung, J. H. Ee, D. Kang, U. R. Kim, J. Lee, and X. P. Wang, Pseudoscalar quarkonium + gamma production at NLL + NLO accuracy, J. High Energy Phys. 10 (2019) 162.
[38] Z. Sun, The studies on $Z \to \Upsilon(1S) + g + g$ at the next-to-leading-order QCD accuracy, Eur. Phys. J. C **80**, 311 (2020).
[39] Z. Sun and H. F. Zhang, Comprehensive studies of Υ inclusive production in Z-boson decay, J. High Energy Phys. 06 (2021) 152.
[40] X. C. Zheng, C. H. Chang, X. G. Wu, X. D. Huang, and G. Y. Wang, Inclusive production of heavy quarkonium ηQ via Z-boson decays within the framework of nonrelativistic QCD, Phys. Rev. D **104**, 054044 (2021).
[41] X. C. Zheng, X. G. Wu, X. J. Zhan, H. Zhou, and H. T. Li, Next-to-leading order QCD corrections to $Z \to \eta_Q + Q + \bar{Q}$, arXiv:2205.03768.
[42] G. Aad *et al.* (ATLAS Collaboration), Search for Higgs and Z-Boson Decays to $J/\psi\gamma$ and $\Upsilon(nS)\gamma$ with the ATLAS Detector, Phys. Rev. Lett. **114**, 121801 (2015).
[43] M. Aaboud *et al.* (ATLAS Collaboration), Searches for exclusive Higgs and Z-boson decays into $J/\psi\gamma$, $\psi(2S)\gamma$, and $\Upsilon(nS)\gamma$ at $\sqrt{s} = 13$ TeV with the ATLAS detector, Phys. Lett. B **786**, 134 (2018).

[44] A. M. Sirunyan *et al.* (CMS Collaboration), Search for rare decays of Z and Higgs bosons to J/ψ and a photon in proton-proton collisions at $\sqrt{s} = 13$ TeV, Eur. Phys. J. C **79**, 94 (2019).

[45] J. B. Guimarães da Costa *et al.* (CEPC Study Group Collaboration), CEPC conceptual design report: Volume 2—physics & detector, arXiv:1811.10545.

[46] J. H. Kuhn and H. Schneider, Inclusive J/ψ's in e^+e^- annihilations, Phys. Rev. D **24**, 2996 (1981).

[47] J. H. Kuhn and H. Schneider, Testing QCD through inclusive J/ψ production in e^+e^- annihilations, Z. Phys. C **11**, 263 (1981).

[48] B. Aubert *et al.* (*BABAR* Collaboration), Observation of the Bottomonium Ground State in the Decay $\Upsilon_{3S} \to \gamma\eta_b$, Phys. Rev. Lett. **101**, 071801 (2008); Erratum, Phys. Rev. Lett. **102**, 029901 (2009).

[49] B. Aubert *et al.* (*BABAR* Collaboration), Evidence for the $\eta_b(1S)$ Meson in Radiative $\Upsilon(2S)$ Decay, Phys. Rev. Lett. **103**, 161801 (2009).

[50] G. Bonvicini *et al.* (CLEO Collaboration), Measurement of the $\eta_b(1S)$ mass and the branching fraction for $\Upsilon(3S) - \to \gamma\eta_b(1S)$, Phys. Rev. D **81**, 031104 (2010).

[51] R. Mizuk *et al.* (Belle Collaboration), Evidence for the $\eta_b(2S)$ and Observation of $h_b(1P) \to \eta_b(1S)\gamma$ and $h_b(2P) \to \eta_b(1S)\gamma$, Phys. Rev. Lett. **109**, 232002 (2012).

[52] A. Petrelli, M. Cacciari, M. Greco, F. Maltoni, and M. L. Mangano, NLO production and decay of quarkonium, Nucl. Phys. **B514**, 245 (1998).

[53] T. Hahn, Generating Feynman diagrams and amplitudes with FeynArts 3, Comput. Phys. Commun. **140**, 418 (2001).

[54] R. Mertig, M. Bohm, and A. Denner, FeynCalc: Computer algebraic calculation of Feynman amplitudes, Comput. Phys. Commun. **64**, 345 (1991).

[55] J. G. Korner, D. Kreimer, and K. Schilcher, A practicable γ_5 scheme in dimensional regularization, Z. Phys. C **54**, 503 (1992).

[56] F. Feng, Apart: A generalized mathematica Apart function, Comput. Phys. Commun. **183**, 2158 (2012).

[57] A. V. Smirnov, Algorithm FIRE: Feynman integral reduction, J. High Energy Phys. 10 (2008) 107.

[58] T. Hahn and M. Perez-Victoria, Automatized one loop calculations in four-dimensions and D-dimensions, Comput. Phys. Commun. **118**, 153 (1999).

[59] B. W. Harris and J. F. Owens, The two cutoff phase space slicing method, Phys. Rev. D **65**, 094032 (2002).

[60] J. X. Wang, Progress in FDC project, Nucl. Instrum. Methods Phys. Res., Sect. A **534**, 241 (2004).

[61] P. A. Zyla *et al.* (Particle Data Group), Review of particle physics, Prog. Theor. Exp. Phys. **2020**, 083C01 (2020).

[62] E. J. Eichten and C. Quigg, Quarkonium wave functions at the origin, Phys. Rev. D **52**, 1726 (1995).